European Conference on Optical Communication (ECOC) 2022 © Optica Publishing Group 2022

Frequency-Selective Phase Noise Cancellation in Photonics-based Radio Frequency Multiplication up to W-band

Antonio Malacarne(1), Antonio D'Errico(2), Alessandra Bigongiari(2), Antonella Bogoni(3,1) and Marco Secondini(3,1)

(1) CNIT - National Inter-University Consortium for Telecommunications, antonio.malacarne@cnit.it
(2) Ericsson Research, Pisa, 56124 Italy
(3) Scuola Superiore Sant'Anna, marco.secondini@santannapisa.it

Abstract *In the case of photonics-based radio frequency multiplication, a method for cancelling the phase noise of the generated carrier at adjustable periodic frequency offset values is proposed, theoretically analyzed, and experimentally demonstrated up to 110 GHz frequency generation from sixfold 18.3 GHz multiplication.*

Introduction

Current and next-generation wireless networks are mainly based on orthogonal frequency division multiplexing (OFDM) [1]–[4] to provide high spectral efficiency and mitigate inter-symbol interference caused by multipath fading. Radio transmission typically takes place in a sub-GHz to sub-THz frequency range [5] and uses high-order modulation formats such as 256 QAM. Unfortunately, OFDM modulated signals are susceptible to phase noise (PN) [6],[7], which induces both a common phase error (CPE) and inter-carrier interference (ICI), whose impact grows as modulation order increases and subcarrier spacing decreases [8],[9]. Simple digital processing techniques can be employed to mitigate CPE, but they are usually ineffective against ICI. The problem is particularly relevant when high-frequency carriers — typically affected by strong PN — are employed.

A convenient solution for the generation and distribution of the required high-frequency carriers is photonics-based radio frequency (RF) multiplication [10]. In this paper, we propose a novel RF multiplication scheme to generate a high-frequency RF carrier, whose PN can be selectively cancelled at periodic frequency offset values. The period can be arbitrarily selected by design. RF generation up to 110 GHz, with PN cancellation at odd multiples of 1 MHz frequency offset is experimentally demonstrated. The scheme can mitigate the impact of ICI in the abovementioned scenario (not demonstrated here) and is partly integrable on CMOS-compatible platform, as shown in [10], except two spools of optical fiber that determine the frequency offset values at which PN is cancelled.

Theoretical analysis

A simple and versatile solution for photonics-based RF multiplication is offered by the scheme depicted in Fig. 1 [10]. The signal can be generated in the optical domain and converted to the mm-band with a remote photodiode (PD), after delivery through optical fiber.

The optical carrier generated by the laser is denoted by

$$E(t) = E_0 \cos(\omega_0 t + \phi_0(t)) \qquad (1)$$

where E_0 is the amplitude, $\omega_0 = 2\pi f_0$ the angular

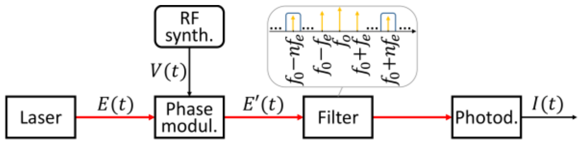

Fig. 1: Photonics-based radio frequency multiplication.

frequency and $\phi_0(t)$ the phase noise (PN) of the laser with power spectral density (PSD) $P_{\phi 0}(f)$. Analogously, the electrical tone generated by the RF synthesizer is denoted by

$$V(t) = V_e \cos(\omega_e t + \phi_e(t)) \qquad (2)$$

It can be shown that the optical signal at the output of the phase modulator is given by

$$E'(t) = E_0 \sum_{k=-\infty}^{\infty} J_k(\beta) \cos\Big((\omega_0 + k\omega_e)t + \phi_0(t) + k\phi_e(t) + k\frac{\pi}{2}\Big) \qquad (3)$$

where $\beta = \pi V_e/V_\pi$, V_π is the half-wave voltage of the modulator and $J_k(\beta)$ is the Bessel function of the first kind of order k [11],[12].

The optical filter then selects only the n-th order optical sidebands, corresponding to the terms with $k = \pm n$ centered at frequencies $f = f_0 \pm nf_e$, as shown in the inset in Fig. 1, obtaining at the PD output

$$I(t) = RE_0^2 J_n^2(\beta) \cos(2n\omega_e t + 2n\phi_e(t)) \qquad (4)$$

where R is the PD responsivity and the DC term (irrelevant and tipically removed by a DC block) is neglected. In practice, the frequency-multiplied RF tone in (4) has $2n$ times the frequency of the original tone generated by the synthesizer, $2n$ times its PN (the electrical PN terms affecting the two selected sidebands are coherently added), whereas it is not affected by the optical PN (the optical PN terms affecting the selected sidebands cancel out). The PSD of the PN of the frequency-multiplied RF tone is therefore

$$P_\phi(f) = (2n)^2 P_{\phi e}(f) \qquad (5)$$

i.e., $(2n)^2$ times the PSD of the electrical PN.

In case a relative delay between the selected optical sidebands is introduced (e.g., by dispersion, as shown in [10]), the coherent combination of the corresponding electrical PN terms can be avoided; on the other hand, the delay would also prevent the exact cancellation of the optical PN terms. Therefore, we propose the alternative scheme of Fig. 2, in which the optical carrier is split and separately processed in two branches by using two modulators, two filters, and two optical delay elements. The different order in which the modulator and the delays are arranged in the lower and upper branches ensures that a relative delay τ is induced only between the corresponding electrical PN terms, while the optical PN terms

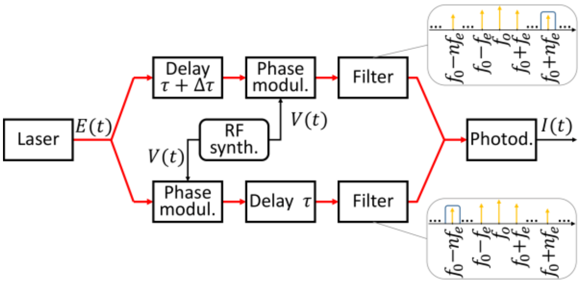

Fig. 2: Photonics-based RF multiplication with frequency-selective PN mitigation.

are kept synchronized (but for a possible delay error $\Delta\tau$), obtaining after optical recombination and photodetection the RF tone

$$I(t) = R\left(\frac{E_0}{2} J_n(\beta)\right)^2 \cos(2n\omega_e t + \phi(t)) \qquad (6)$$

where we have defined the overall PN term

$$\begin{aligned}\phi(t) = n\big(\phi_e(t) + \phi_e(t-\tau)\big) \\ + \phi_0(t-\tau-\Delta\tau) \\ - \phi_0(t-\tau)\end{aligned} \qquad (7)$$

with PSD

$$\begin{aligned}P_\phi(f) = (2n)^2 \cos^2(\pi f \tau)\, P_{\phi e}(f) \\ + 4\sin^2(\pi f \Delta\tau)\, P_{\phi 0}(f)\end{aligned} \qquad (8)$$

Compared to the PSD in (5), obtained with the conventional scheme of Fig. 1, the impact of the electrical PN in (8) is mitigated by the cos^2 term, which periodically vanishes at frequencies

$$f_m = (m + 1/2)/\tau \qquad (9)$$

with m integer. On the other hand, the presence of a possible delay error $\Delta\tau$ prevents the full cancellation of the optical PN, whose contribution shows up at high frequency. It is therefore possible to select the frequency values at which the PN is cancelled by properly setting τ. At the same time, it is crucial to make the delay error $\Delta\tau$ small enough to keep the contribution of the optical PN negligible, e.g., by making sure the sin^2 term remains small up to the frequency where $P_{\phi 0}(f)$ becomes also sufficiently small. An example will be shown in the next section.

Experimental implementation and results

The scheme depicted in Fig. 2 has been experimentally implemented to demonstrate the frequency-selective PN cancellation concept applied to a W-band carrier frequency generation.

The employed laser is an external cavity laser with emission wavelength of 1549 nm, output power of 13 dBm and typical linewidth ≤100 kHz. Light is split into two branches through an optical splitter with input/output polarization-maintaining standard single-mode fiber (PM-SMF). In the lower branch, a Lithium Niobate ($LiNbO_3$) phase modulator with PM-SMF pigtails is driven by the output of an electrical synthesizer employed as the reference clock, set at a frequency of 18.75 GHz, after RF amplification up to a 27-dBm power. The modulator is then followed by a 100 meters-long PM-SMF spool implementing a delay $\tau \sim 500$ ns. In the upper arm, another $LiNbO_3$ phase modulator, driven in the same way, is preceded by a spool of PM-SMF of equal length. Each phase modulator acts as an optical frequency comb (OFC) generator with a free spectral range (FSR) equal to the driving reference frequency [10]. One optical line out of the generated OFC at each phase modulator output is then selected by a liquid-crystal on Silicon (LCoS) WaveShaper (WS), acting as a programmable optical filter. This way, a suppression of adjacent lines no lower than 48 dB is guaranteed. The two WSs outputs are then combined through an SMF optical coupler. The RF tone resulting from the beating of the two selected optical modes is finally obtained at the output of a high-speed photodiode (PD) with a 3 dB-bandwidth of 100 GHz. The PN PSD of the generated RF carrier is then measured with a signal source analyzer (SSA). Fig. 3 shows the optical spectrum at each of the two WSs' outputs, together with each corresponding generated OFC, for fourfold frequency multiplication ($n = 2$). The filter guarantees a rejection of more than 40dB of each adjacent sideband compared to the selected one. Fig. 3(c) shows (green) the

European Conference on Optical Communication (ECOC) 2022 © Optica Publishing Group 2022

spectrum before the PD, after recombination of the two branches.

The measured PN PSDs shown in Fig. 4 excellently confirm the theoretical analysis. In one case a single branch of the scheme is connected and the WS selects the two 75 GHz-

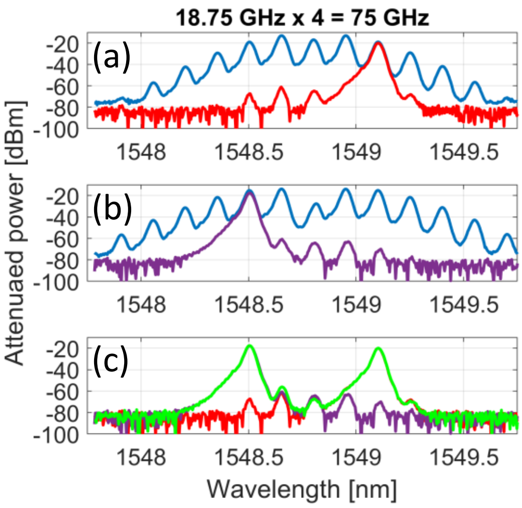

Fig. 3: Optical spectrum at the filter output for upper (a) and lower (b) branch, together with the corresponding generated OFC (blue). Optical spectrum after recombination (c).

spaced optical lines, as in the scheme of Fig. 1, leading to the yellow curve. When employing the complete scheme with $\tau \sim 500$ ns (orange plot), the PN PSD generally follows the single-branch case (yellow line) but gets cancelled at frequency offsets equal to ~ 1 MHz, 3MHz, 5MHz etc., in agreement with (9), except for the frequency range $f \leq 15$ kHz. Indeed, long optical delay lines induce thermal and mechanical instabilities, leading to a time-varying phase shift between the optical signals traveling in the two branches, causing an additional PN term to appear in (7).

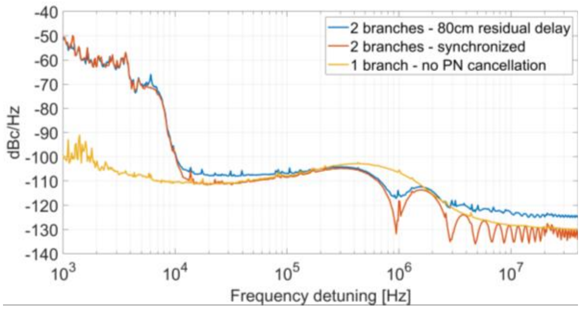

Fig. 4: PN PSD of the generated 75 GHz frequency, in case of single-branch configuration (yellow), complete scheme with $\tau \sim 500$ ns (orange) and with a residual $\Delta\tau \sim 4$ ns (blue).

However, such a contribution is limited to the low-frequency part of the PSD and is usually negligible in most applications. The last curve in Fig. 4 shows the impact of a delay mismatch $\Delta\tau \sim 4$ ns between the two branches. The increase of the PSD with respect to the case $\Delta\tau \sim 0$ is due to the second term in (8), which shows up when the last two terms in (7) do not cancel out.

As a last result, Fig. 5 shows the measured PN PSD in case of sixfold RF multiplication, generating a 110 GHz RF carrier. The behavior is similar to the case in Fig. 4, but for a lower measurement sensitivity, which makes the PN cancellation at high frequency less noticeable. This is caused by a lower optical power of the selected spectral lines, clearly appreciable by comparing Fig. 6 with Fig. 3(c). Indeed, to compensate for the high loss introduced by the external harmonic mixers required to down-convert the signal before PN analysis at the SSA, optical amplification is included before the PD and the resulting lower optical signal-to-noise ratio ultimately determines such sensitivity level.

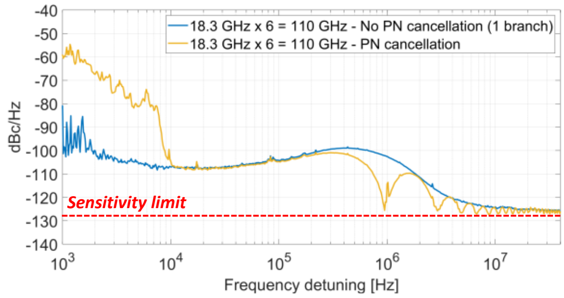

Fig. 5: PN PSD of generated RF carrier at frequency 110 GHz in case of single-branch configuration (blue) and with the complete scheme and $\tau \sim 500$ ns (yellow).

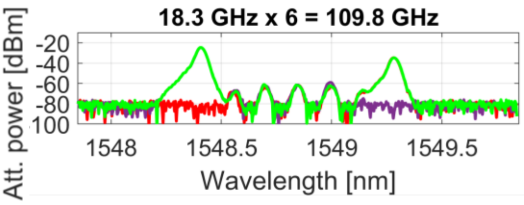

Fig. 6: Optical spectrum after recombination in case of generation of 110 GHz.

Conclusions

A new method for tailored mitigation of phase noise (PN) in photonics-based RF multiplication has been proposed and experimentally verified. RF carriers at 75 GHz and 110 GHz have been generated by fourfold multiplication of an 18.75 GHz carrier and sixfold multiplication of an 18.3 GHz carrier, respectively. In both cases, the PSDs of the generated carriers vanish at frequency offset values that are odd multiples of 1 MHz, confirming the selective PN cancellation predicted by theory.

Acknowledgements

This work is supported by the Italian Ministry of Education, Universities and Research (FISR program) through COSMOS project, and by the European Union's Horizon 2020 research and innovation programme under grant agreement No. 863322 (TERASLICE project).

Disclaimer: Preliminary paper, subject to publisher revision

European Conference on Optical Communication (ECOC) 2022 © Optica Publishing Group 2022

References

[1] 3GPP, “3GPP Home Page.” [Online]. Available: https://www.3gpp.org/

[2] 5GPP, “5GPP Home Page” [Online]. Available: https://5g-ppp.eu/

[3] "IEEE Standards Association." [Online]. Available: https://www.ieee802.org/11/

[4] "IEEE Standards Association." [Online]. Available: https://standards.ieee.org/ieee/802.16/

[5] A. Osseiran, J. F. Monserrat, P. Marsch, Patrick, "5G Mobile and Wireless Communications Technology", Cambridge University Press, 2016

[6] A. G. Armada and M. Calvo, "Phase noise and sub-carrier spacing effects on the performance of an OFDM communication system," IEEE Communications Letters, vol. 2, no. 1, pp. 11–13, Jan 1998. DOI: 10.1109/4234.658613

[7] A. G. Armada, "Understanding the effects of phase noise in orthogonal frequency division multiplexing (OFDM)," IEEE Transactions on Broadcasting, vol. 47, no. 2, pp. 153–159, Jun 2001. DOI: 10.1109/11.948268

[8] P. Robertson and S. Kaiser, "Analysis of the effects of phase-noise in orthogonal frequency division multiplex (OFDM) systems," Proceedings IEEE International Conference on Communications ICC '95, 1995, pp. 1652-1657 vol.3, DOI: 10.1109/ICC.1995.524481.

[9] A. Leshem and M. Yemini, "Phase Noise Compensation for OFDM Systems," in IEEE Transactions on Signal Processing, vol. 65, no. 21, pp. 5675-5686, 1 Nov.1, 2017. DOI: 10.1109/TSP.2017.2740165

[10] A. Malacarne, F. Falconi, A. Bigongiari, A. D'Errico, A. Bogoni and C. Porzi, "Reconfigurable Low-Phase Noise Frequency Generation up to 92.5 GHz in a Monolithically Integrated Silicon Photonics Circuit," 2021 European Conference on Optical Communication (ECOC), 2021. DOI: 10.1109/ECOC52684.2021.9605957

[11] G. Qi, J. Yao, J. Seregelyi, S. Paquet, C. Bélisle, X. Zhang, K. Wu, and R. Kashyap, “Phase-noise analysis of optically generated millimeter wave signals with external optical modulation techniques,” in Journal of Lightwave Technology, vol. 24, no. 12, pp. 4861-4875, Dec. 2006, DOI: 10.1109/JLT.2006.884990.

[12] M. Abramowitz and I. A. Stegun, Handbook of mathematical functions with formulas, graphs, and mathematical tables, vol. 55 (US Government printing office, 1972)